RESEARCH PAPER

Synthesis of Indenopyrazolones Using Functionalized SBA-15

Hossein Shahbazi-Alavi[1*], Atefeh Bakhtiari [2], Javad Safaei-Ghomi [2],Sheida Khojasteh-Khosro [2]

[1] Young Researchers and Elite Club, Kashan Branch, Islamic Azad University, Kashan, Iran

[2] Department of Organic Chemistry, Faculty of Chemistry, University of Kashan, Iran

ARTICLE INFO

Article History:
Received 01 December 2020
Accepted 28 January 2021
Published 15 March 2021

Keywords:
Nanocatalyst
SBA-15
Nanochemistry
Indenopyrazolones

ABSTRACT

Functionalized SBA-15 (immobilization of Pd on modified SBA-15) has been applied as an efficient catalyst for the preparation of indenopyrazolones by the multi-component reactions of phenylhydrazine, aromatic aldehydes, and indan-1,2,3-trione at room temperature in acetonitrile. The catalyst has been characterized by X-ray diffraction spectroscopy (XRD), field emission scanning electron microscopy (FE-SEM), transmission electron microscopy (TEM), X-Ray photoelectron spectroscopy (XPS), energy-dispersive X-ray spectroscopy (EDX), Fourier-transform infrared spectroscopy (FT-IR), N2 adsorption analysis, temperature-programmed desorption (TPD), and differential thermal analysis (TGA-DTA). This method has a number of merits including the reusability of the catalyst, low catalyst loading, excellent yields in short reaction times, and easy separation of products.

How to cite this article
Shahbazi-Alavi H., Bakhtiari A., Safaei-Ghomi J., Khojasteh-Khosro Sh. Synthesis of Indenopyrazolones Using Functionalized SBA-15. Nanochem Res, 2021; 6(1):53-64. DOI: 10.22036/ncr.2021.01.005

INTRODUCTION

Pyrazolones demonstrate important biological properties such as being anticancer [1], antibacterial [2], anti-inflammatory [3], antioxidant [4] and analgesic [5]. Indenopyrazoles display antidiabetic [6], antimicrobial [7], antitumor [8], and anticonvulsant [9] activities. Indeno-fused heterocycles have attracted considerable attention from both medicinal and synthetic chemists in recent years [10-12]. These attributes make pyrazolones a noteworthy target in organic synthesis. A number of ways have been improved for the preparation of pyrazolones in the presence of such catalysts as acetic acid [13], [HMIM]HSO_4 [14], 3-aminopropylated silica gel [15], sodium dodecyl sulfate [16] silica-bonded S-sulfonic acid [17], and Ce/SiO_2 composite [18]. While the development of each of these methods has contributed to moving the field forward, some of them suffer such drawbacks as prolonged reaction times, complicated work-up, low yields, and hazardous reaction conditions. Therefore, in order to avoid these drawbacks, finding an effective way for the preparation of indenopyrazolones is still favored. Microporous materials with regular-pore frameworks are a good choice for immobilizing ligands [19]. An improved understanding of the efficiency of ordered mesoporous silica (OMS) could be obtained by evaluating their potential applications in drug delivery, separation, gas storage, catalysis, and biomolecules [20]. SBA-15 was employed due to its properties such as large pore volume, uniform-sized pores, high specific surface area, and thermal and hydrothermal stability [21]. The anchoring of a wide range of organic functional groups to the pore surface of SBA-15 improves the catalytic ability [22]. A stable attachment of ligand could be reached by post-synthetically available ligand precursors to SBA-15 [23]. We report herein the use of functionalized SBA-15 as an effective catalyst for the preparation of indenopyrazolones by the multi-component reactions of phenylhydrazine, aromatic aldehydes and indan-1,2,3-trione at room temperature in acetonitrile (Scheme 1).

* Corresponding Author Email: *hossien_shahbazi@yahoo.com*

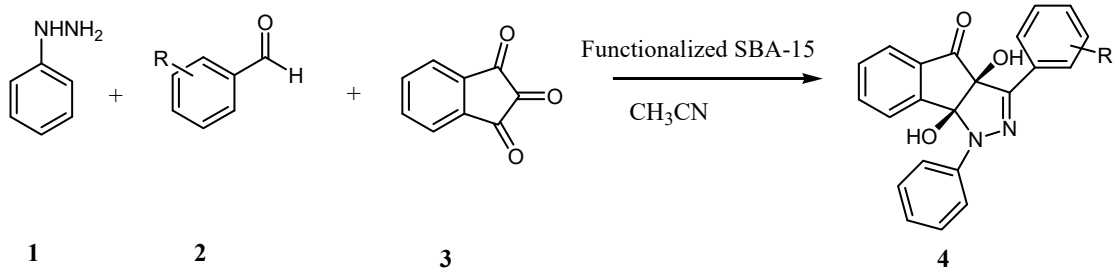

Scheme 1. Synthesis of indenopyrazolones catalyzed by Functionalized SBA-15

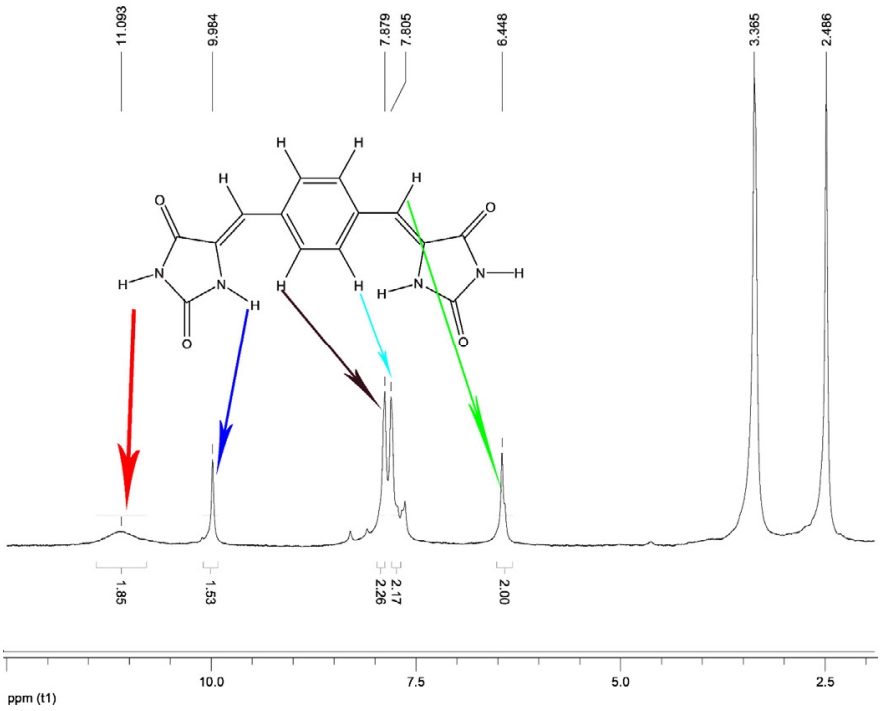

Fig. 1. H NMR of ligand (imidazolidone) DMSO

EXPERIMENTAL SECTION

Preparation of Ligand (imidazolidone)

In a 50 ml round-bottom flask, 4 mmol of hydantoin was dissolved in 4 mL water. Then an amount of saturated sodium hydrogen carbonate solution was added and the pH of the reaction mixture was maintained at 7.0. After that, ethanolamine (0.36 mL) was added, and the solution was warmed up gradually to 90 ˚C. A solution of terephthaldehyde (4 mmol) in 4 mL of ethanol was added dropwise. Then the mixture was continuously stirred for 48 hrs at 120 ˚C and kept under reflux. A precipitate was formed by cooling in an ice-salt bath at about 0 ˚C. It was filtered and washed with H_2O/EtOH 5:1. The structure of ligand (imidazolidone) was confirmed by ^{1}H NMR and FT-IR spectrum presented in Figs. 1 and 5, respectively.

Preparation of SBA-15 nanostructure

The hexagonal pore structure of SBA-15 has been produced using pluronic 123 triblock copolymers (EO20–PO70–EO20) by the procedure as reported in the previous paper [24].

Preparation of 3-chloropropyltriethoxysilane attached to SBA-15 (chlorinated-SBA-15)

In a 50 mL round-bottom flask, 3 mmol of 3-chloropropyltriethoxysilane and 1 g of calcined SBA-15 were suspended in dry toluene and refluxed

at 80 ˚C under an inert atmosphere for 24 hrs. Then, the solid was filtered and washed successively with ethanol. Finally, a white powder was dried under vacuum at 70 ˚C for 8 hrs to generate the 3-chloropropyltriethoxysilane attached to SBA-15 (Cl-modified SBA-15).

Preparation of modified SBA-15 (Immobilization of ligand (imidazolidone) to chlorinated-SBA-15)

The solution of ligand (imidazolidone) (2 mmol) in dimethylformamide (10 mL) was added at 60% suspension of sodium hydride. The resulting mixture was stirred for 60 minutes. Then chloro-modified SBA-15 (4.5 g, 26.3 mmol) was added to the reaction mixture. The solution was warmed up gradually to 80 ˚C and stirred for 18 hrs. The reaction was quenched with 1 N HCl (20 mL, 20 mmol) and the precipitated solid was collected by centrifugation, and then a pure product was obtained by washing with EtOH to produce modified SBA-15 (immobilization of ligand (imidazolidone) to chlorinated-SBA-15).

Preparation of Immobilization of Pd on the modified SBA-15 (catalyst)

To a suspension of modified SBA-15 (1 g) in dry ethanol (20 mL), 0.1 g of $PdCl_2$ was added and the solution was refluxed for 3 hrs. The yellow light solid was separated by centrifuging and was dried afterwards. Unreacted palladium from the surface was removed using Soxhlet extracted with acetone.

Synthesis of indenopyrazolones

A mixture of phenylhydrazine (1.0 mmol), benzaldehydes (1.0 mmol), ninhydrin (1.0 mmol), and 6 mg functionalized SBA-15 (catalyst) in acetonitrile (10 mL) was stirred for the appropriate times. The reaction was monitored by TLC (*n*-hexane/ethyl acetate 7:3). After the completion of the reaction, the catalyst was recycled by a simple filtration. The catalyst was washed with a small amount of hot ethanol, dried in an oven at 80 °C for 6 hours, and then reused for the next run as indicated above for the model reaction. The solvent was evaporated using a rotary evaporator and the residue was washed with cold diethyl ether to get pure product. The characterization data of the compounds are presented below.

cis-3a,8b-Dihydro-3a,8b-dihydroxy-1,3-diphenylindeno[1,2-c]pyrazol-4(1H)-one (**4a**): Yellow solid; Mp. 221-223 °C, IR (KBr): νmax = 3435, 3053, 1736, 1458 cm^{-1}. ^1H NMR (400 MHz, $CDCl_3$): δ (ppm) = 6.12 (s, OH); 6.17 (s, OH); 7.15 (d, *J* = 8.0 Hz, 1H, ArH); 7.18-7.30 (m, 3H, ArH); 7.40 (t, *J* = 7.6 Hz, 1H, ArH); 7.48 (t, *J* = 7.6 Hz, 1H, ArH); 7.52–7.66 (m, 5H, ArH); 8.22 (d, *J* = 7.6 Hz, 2H, ArH); 8.48 (d, *J* = 7.6 Hz, 1H, ArH). ^{13}C NMR (100 MHz, $CDCl_3$): δ (ppm) = 89.2 (C); 96.9 (C); 118.2 (2 CH); 121.4 (CH); 122.6 (CH); 123.2 (CH); 124.0 (CH); 126.2 (2 CH); 129.5 (2 CH); 130.7 (CH); 130.8 (C); 132.8 (2 CH); 133.5 (CH); 137.2 (C); 139.8 (C); 142.3 (C); 147.8 (C); 196.7 (C=O). Analysis for $C_{22}H_{16}N_2O_3$: calcd. C, 74.15; H, 4.53; N, 7.86%; Found C, 74.12; H, 4.56; N, 7.90%.

cis-3a,8b-Dihydro-3a,8b-dihydroxy-3-(4-methoxyphenyl)-1-phenylindeno[1,2-c]pyrazol-4(1H)-one (**4b**): Yellow solid; Mp. 211-214 °C, IR (KBr): νmax = 3422, 3282, 1702, 1592 cm^{-1}. ^1H NMR (400 MHz, $CDCl_3$): δ (ppm) = 3.65 (s, OCH_3); 6.12 (s, OH); 6.23 (s, OH); 6.88 (d, *J* = 8.2 Hz, 2H, ArH); 7.05 (t, *J* = 7.2 Hz, 1H, ArH); 7.18 (t, *J* = 7.4 Hz, 2H, ArH); 7.27 (t, *J* = 7.2 Hz, 1H, ArH); 7.37 (t, *J* = 7.4 Hz, 1H, ArH); 7.50 (d, *J* = 7.8 Hz, 1H, ArH); 7.55 (d, *J* = 7.4 Hz, 1H, ArH); 7.60 (d, *J* = 7.8 Hz, 2H, ArH); 8.02 (d, *J* = 8.4 Hz, 2H, ArH). ^{13}C NMR (100 MHz, $CDCl_3$): δ (ppm) = 55.4 (OCH_3); 90.1 (C); 96.5 (C); 113.7 (2 CH); 117.8 (2 CH); 122.3 (CH); 123.7 (CH); 124.3 (C); 125.8 (CH); 128.6 (2 CH); 129.3 (2 CH); 130.4 (CH); 135.3 (C); 136.7 (CH); 142.8 (C); 143.3 (C); 147.7 (C); 160.4 (C); 197.5 (C=O). Analysis for $C_{23}H_{18}N_2O_4$: calcd. C, 71.49; H, 4.70; N, 7.25%; Found C, 71.36; H, 4.60; N, 7.17%.

RESULTS AND DISCUSSION

Scheme 2 shows preparation of the immobilization of Pd on modified SBA-15 (catalyst).

The structure of ligand (imidazolidone) was confirmed by ^1H NMR and FT-IR spectrum presented in Figs. 1 and 5, respectively.

The effect of modification on the structural framework of SBA-15 is monitored by a small-angle X-ray diffraction method (Fig. 2). A significant degree of long-range ordering of the structure has been determined by an intense diffraction peak (1 0 0). Two secondary high order peaks with lower intensities corresponding to (1 1 0) and (2 0 0) approve 2D-hexagonal planes of the mesoporous [25]. On modification with ligand and metal, the intensities of the peaks are decreased which can be due to silylation inside the mesopores of SBA-15. The presence of similar peaks for Pd@modified SBA-15 indicates that the structural ordering of SBA-15 is not diminished during the silylation

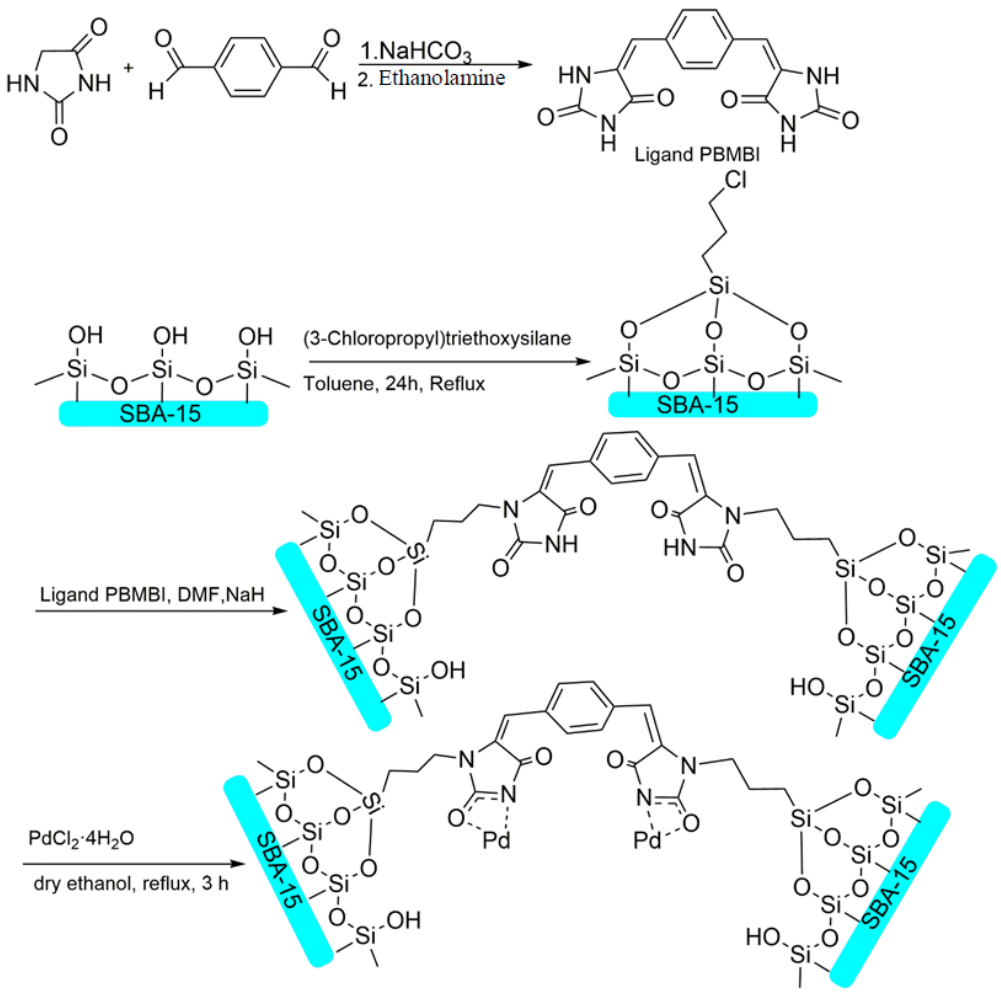

Scheme 2. Different steps for synthesis of immobilization of Pd on modified SBA-15 (Pd@modified SBA-15).

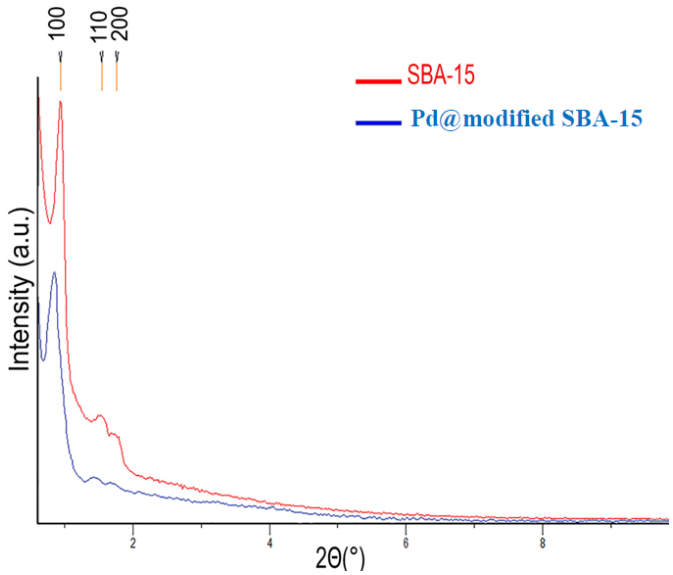

Fig. 2. The XRD pattern of SBA-15 and Pd@modified SBA-15

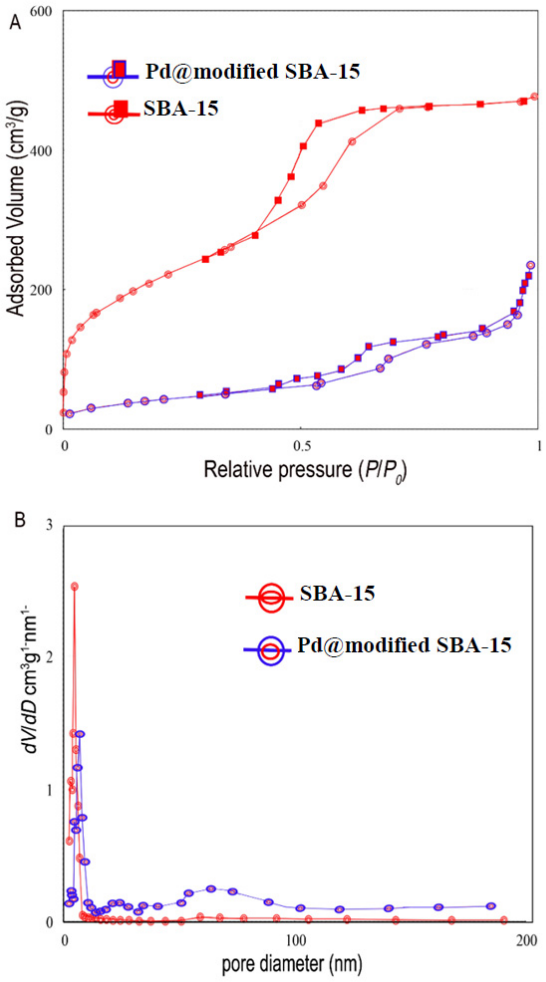

Fig. 3. N2 adsorption-desorption isotherms and pore size distributions of SBA-15, Pd@modified SBA-15

Table 1. Structural and Textural Parameters of SBA-15 and Pd@modified SBA-15

Entry	Sampel	*S* BET[a] [m^2 g^{-1}]	D_p[b] [nm]	V_P[c] [cm^3 g^{-1}]
1	SBA-15	758.68	9.40	0.7378
2	Pd/PBMBI-SBA-15	161.89	7.59	0.3587

[a] *S* BET = surface area. [b] *D*p = average pore width. [c] *V*p = total pore volume.

procedure. The 2D-hexagonal structure of SBA-15 is also preserved regardless of the ligand and metal loading.

The porous structure of SBA-15 and Pd@ modified SBA-15 are analyzed by N2 sorption isotherms and pore size distributions (Fig. 3). Type IV adsorption-desorption isotherm with an H1 hysteresis loop is observed for both of them which can be characterized as mesoporous solids [26]. The isotherm of Pd@modified SBA-15 indicates a lower N2 uptake, related to a diminution in pore volume and the specific surface area (Table 1). The height of the capillary condensation step slightly reduces due to pore blocking effect by changing in pore size distribution. Indeed, less uniformity of the mesopore size distribution is visible in functionalized SBA-15.

The FESEM of SBA-15 and Pd@modified SBA-15 manifest structural integrity and morphology (Fig. 4 a,b). The integrity of the porous structure

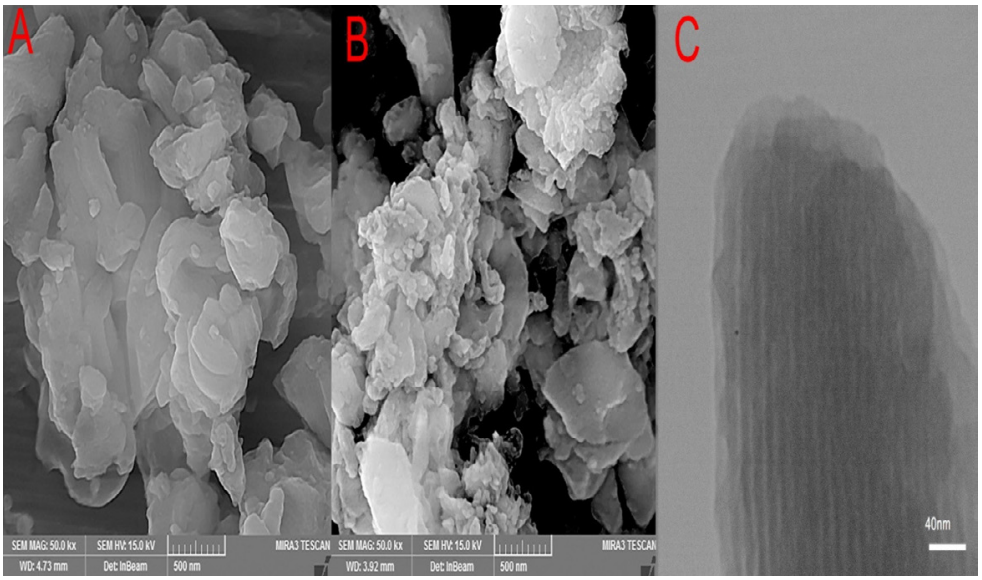

Fig. 4. SEM images of (A) SBA-15 and (B) Pd@modified SBA-15 (C) TEM image of Pd@modified SBA-15

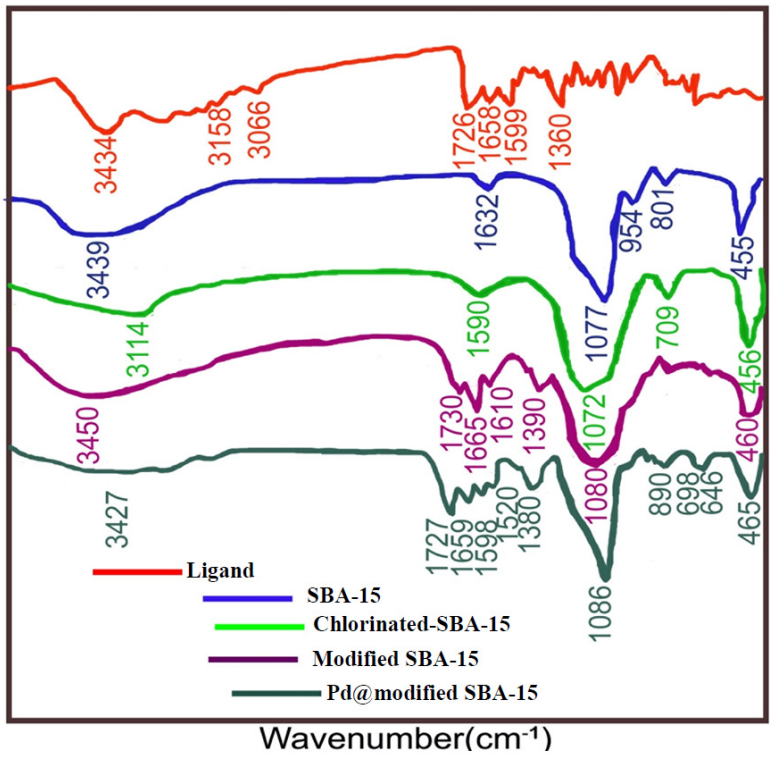

Fig. 5. FT-IR spectra of ligand, SBA-15, chlorinated-SBA-15, modified SBA-15, Pd@modified SBA-15

of SBA-15 is preserved after loading Palladium and ligand. 2D Hexagonal network of the Pd@modified SBA-15 is determined by the TEM image that shows parallel channels (Fig. 4 c).

From the FT-IR spectra (Fig. 5), the SBA-15 spectrum displays a broad absorption band at 3439 cm^{-1} which is associated with the presence of silanol groups. A low-intensity band at 1632 cm^{-1} is attributed to the deformation modes of O-H bonds from adsorbed water. The Si-O-Si bond stretching

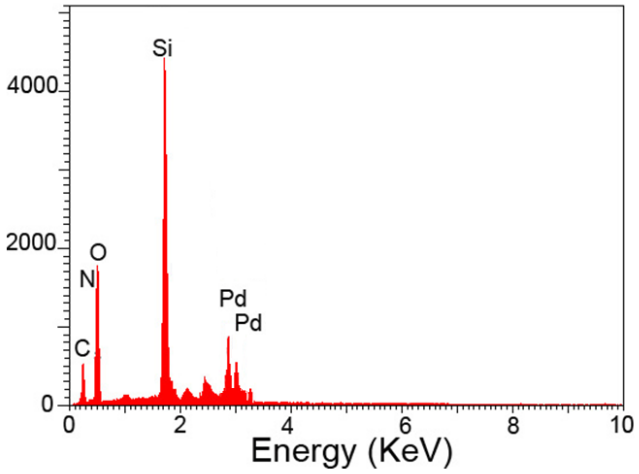

Fig. 6. EDX spectrum of Pd@modified SBA-15

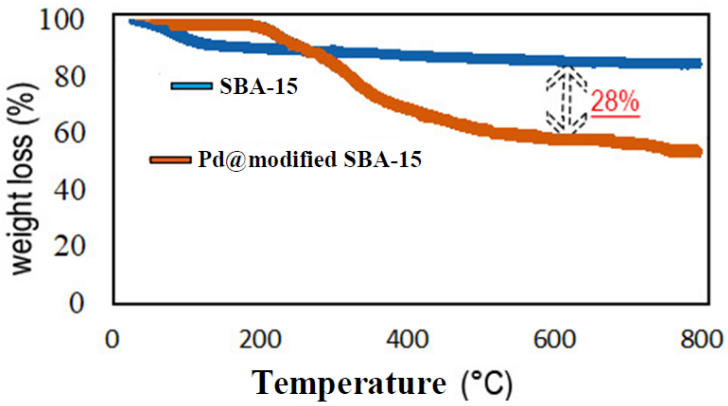

Fig. 7. TGA and DTA curves of SBA-15 and Pd@modified SBA-15

vibrations with the bending vibrations are revealed at 1077 cm^{-1}, 801 cm^{-1}, and 455 cm^{-1}. The stretching vibrations of the Si-OH and Si-O-Si bonds appear as a weak band at 960 cm^{-1}. The peaks related to silica network of SBA-15 are observed with the same intensity in all processes of functionalization. In the spectrum of chlorinated-SBA-15, peaks at 3114 cm^{-1} and 1590 cm^{-1} are associated with the vibration of C–H bond in the propyl group. A peak at 709 cm^{-1} can be attributed to the C-Cl bonds. The results of the ^1H NMR spectrum of ligand are approved by FT-IR spectrum. The FT-IR spectrum of ligand exhibits three sharp peaks at 1730, 1665 and 1610 cm^{-1} attributed to the C=O and C=C bonds, respectively. Moreover, the absorption band at 3450 cm^{-1} is attributed to the NH stretching vibrations. By loading Pd, the intensity of the absorption band at 3450 cm^{-1} has diminished and slightly moved towards the lower frequency region. The absorption band at 1520 cm^{-1} has appeared due to ring >C=N stretching vibration. Based on the results, the complexion of Pd ions with modified SBA-15 has been approved.

The peaks of carbon, nitrogen, oxygen, silicon, and palladium became visible in the EDX spectra which confirmed the uniform distribution of ligand and palladium over SBA-15 (Fig. 6). The weight percentages of elements calculated by EDX are: C (21.97%), N (5.75%), O (46.90%), Si (20.80%), Pd (4.58%).

The TGA analysis demonstrates that Pd@ modified SBA-15 has higher weight loss than that of neat SBA-15 (Fig. 7). The weight loss was measured at about 28% up to 300 °C in two steps: the removal of physically absorbed water in the first step and, in the second step, the thermal decomposition of

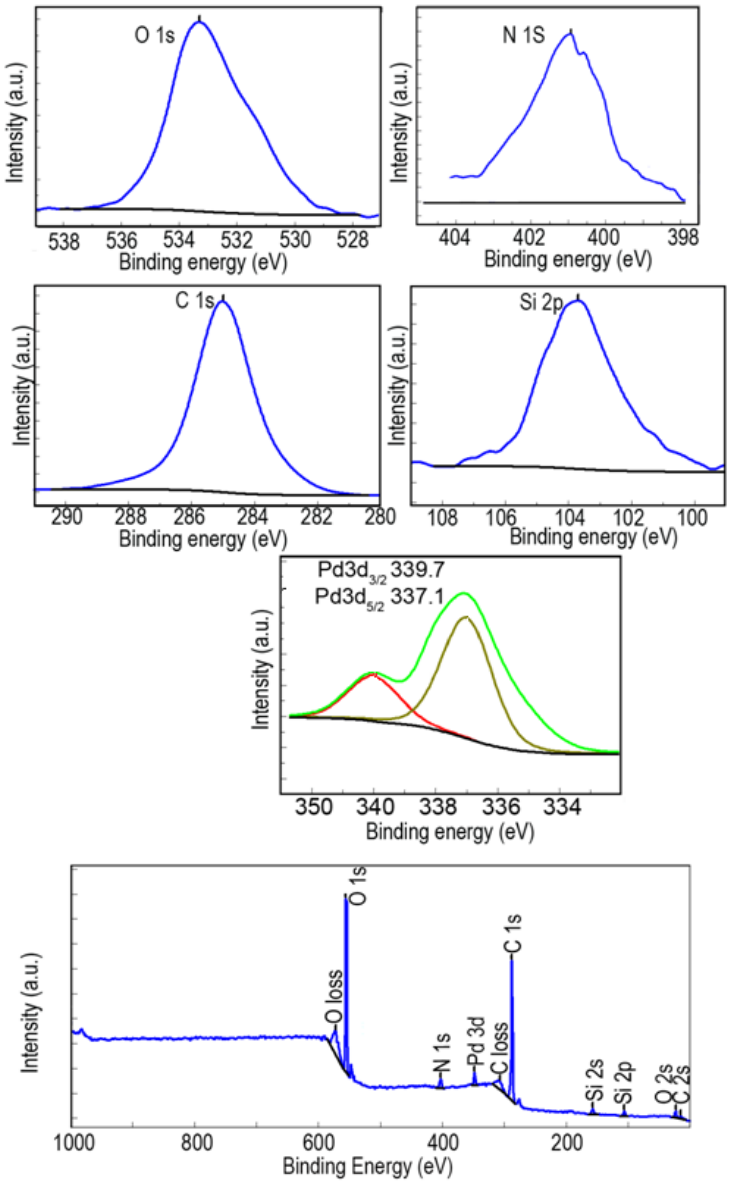

Fig. 8. XPS spectra of O 1s, N 1s, C 1s, Si 2p, Pd 3d and Pd@modified SBA-15

the organic functional group which starts above 300 °C. Consequently, the high decomposition temperature (above 300 °C) is evidence of the high thermal stability of complex Pd/ligand.

The atomic concentration of catalyst and electronic state of the palladium has been characterized by X-Ray photoelectron spectroscopy (Fig. 8). N 1s, C 1s, and Pd 3d peaks are found on the side of Si 2s, Si 2p, and O 1s peaks that approve the loading of ligand and metal on the SBA-15 surface. The N 1s spectrum of Pd@modified SBA-15 shows a peak at 401 eV due to σ*(N-H) resonance. Also, a shoulder is observed at 400 eV which may be caused by π*(NHC=O). Amide π* resonances occur at very similar energies as the σ*(N–H) resonance. The intense and broad C 1s spectrum has exhibited a peak at 285 eV for C–Si, C–H*, σ*(C–C), and σ*(C–N) resonances [27]. The presence of the SiO_2 structure is confirmed by binding energies at 103 and 150 eV for Si 2s and Si 2p, respectively [28]. The binding energy of O 1s is 533.52 eV which could be assigned to Si-O, C-O, and C=O. Two distinct peaks at 337.1 and 339 eV have been observed in Pd 3d spectrum of Pd@modified SBA-15 which

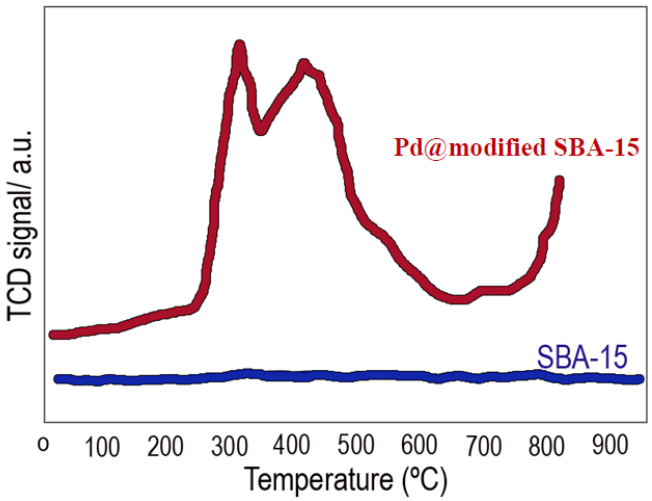

Fig. 9. NH_3-TPD spectra of SBA-15 and Pd@modified SBA-15

Table 2. Optimization of reaction conditions using different catalysts [a]

Entry	Catalyst (amount)	Solvent	Time (min)	Yield[a] %
1	none	CH_3CN	250	16
2	Et_3N (5 mol%)	CH_3CN	200	22
3	nano-NiO (5 mol%)	CH_3CN	200	46
4	*p*-TSA (8 mol%)	CH_3CN	200	35
5	Ligand (5 mol%)	CH_3CN	200	41
6	SBA-15 (5 mol%)	CH_3CN	150	50
7	modified SBA-15 (8 mg)	CH_3CN	100	64
8	Pd@modified SBA-15 (4 mg)	CH_3CN	30	83
9	Pd@modified SBA-15 (6 mg)	CH_3CN	30	92
10	Pd@modified SBA-15 (8 mg)	CH_3CN	30	92
11	Pd@modified SBA-15 (8 mg)	H_2O	150	66
12	Pd@modified SBA-15 (8 mg)	DMF	100	72
13	Pd@modified SBA-15 (8 mg)	EtOH	70	80

[a] Phenylhydrazine (1 mmol) , benzaldehyde (1 mmol), and indan-1,2,3-trione (1 mmol)
[b] Isolated yield

is associated with 3d 5/2 and 3d 3/2, respectively. Atomic percentage concentrations of the Pd@ modified SBA-15 calculated by XPS: C (77.58), N (6.87), O (9.41), Si (5.42), Pd(0.15).

NH_3-TPD analysis has been used to calculate the surface acidity of the catalyst (Fig. 9). The TPD curve of initial SBA-15 exhibits no peaks that determined SBA-15 material has no acidity. The immobilization of Pd/ligand complex leads to improving the acidity of the catalyst as opposed to the initial SBA-15. The TPD curve of Pd@modified SBA-15 represents a sharp peak at 300 °C and a peak around 450 °C correlated with weak and medium acid sites, respectively. Also, there is a shoulder peak at ca. 550 °C that is attributed to strong acid sites. Indeed, there are some weak, medium, and strong acid sites in the Pd@modified SBA-15 that make it a very effective catalyst.

Using the reaction of phenylhydrazine, benzaldehyde, and indan-1,2,3-trione as a model procedure, we conducted it in the presence of Et_3N, *p*-TSA nano-NiO, Ligand, SBA-15, modified SBA-15, and Pd@modified SBA-15. The results are summarized in Table 2. We found that the reaction gave very useful results in the presence of Pd@modified SBA-15 (6 mg for a 1 mmole scale reaction) in acetonitrile at room temperature. Furthermore, we conducted the reaction of

Table 3. Synthesis of indenopyrazolones

Entry	R	product	Time (min)	Yield (%)[b]	m.p. found (°C)
1	H	**4a**	30	92	221-223
2	4-OMe	**4b**	45	84	211-214
3	4-Me	**4c**	45	86	249-251
4	4-Cl	**4d**	25	94	234-236
5	4-Br	**4e**	25	94	222-224
6	4-NO_2	**4f**	25	96	242-244
7	3- NO_2	**4g**	30	93	240-243
8	4-OH	**4h**	50	82	202-204

[a] Phenylhydrazine (1 mmol) , aromatic aldehydes (1 mmol), and indan-1,2,3-trione (1 mmol)
[b] isolated yield

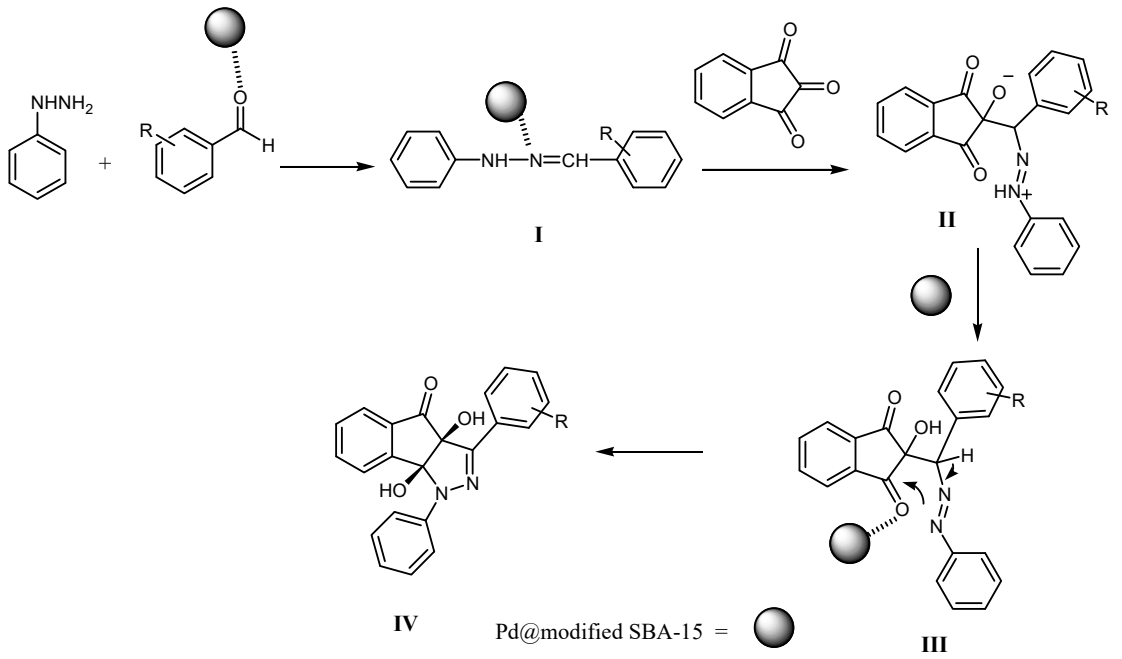

Scheme 3. Proposed mechanism for the synthesis of indenopyrazolones

phenylhydrazine and indan-1,2,3-trione with other aromatic aldehydes and consistently found satisfactory results (Table 3). Yields were slightly higher for aldehydes substituted with electron-withdrawing groups.

The reusability of our nanocatalyst was examined for the model reaction, and it was found that product yields lessened only to a very small extent on each reuse (run 1, 92%; run 2, 92%; run 3, 91%; run 4, 91%; run 5, 90%; run 6, 90%).

Scheme 3 shows a plausible mechanism for this process in the presence of Pd@modified SBA-15. At the start, the activated aldehyde by Pd@modified SBA-15 is condensed with the phenylhydrazine to give intermediate I, which attacks indan-1,2,3-trione to afford the zwitterionic intermediate II. Its tautomer III undergoes an intramolecular nucleophilic addition reaction, which affords the product by an H-atom-transfer reaction. A highly regiospecific synthesis and crystal structure of

indenopyrazolone was reported by Yavari and coworkers [29]. The *cis* configuration of the hydroxy groups was confirmed by NMR (both –OH groups are involved in intramolecular H-bond and X-Ray crystal) [29-31].

CONCLUSIONS

In conclusion, we have reported an efficient procedure for the synthesis of indenopyrazolones through a three-component reaction involving phenylhydrazine, aromatic aldehydes and indan-1,2,3-trione. Our procedure uses Pd@modified SBA-15 at room temperature in acetonitrile. The catalyst has been characterized by XRD, FE-SEM, TEM, EDX, XPS, FT-IR, N_2 adsorption analysis, TPD, and TGA-DTA. Very satisfactory yields, the excellent reusability of the catalyst, low catalyst loading, and easy separation of products are the merits of this method.

CONFLICTS OF INTEREST

The authors announce that there are no conflicts of interest.

REFERENCES

1. Saidachary G, Veera Prasad K, Divya D, Singh A, Ramesh U, Sridhar B, et al. Convenient one-pot synthesis, anti-mycobacterial and anticancer activities of novel benzoxepinoisoxazolones and pyrazolones. European Journal of Medicinal Chemistry. 2014;76:460-9.
2. Indrasena A, Riyaz S, Mallipeddi PL, Padmaja P, Sridhar B, Dubey PK. Design, synthesis, and biological evaluation of indolylidinepyrazolones as potential anti-bacterial agents. Tetrahedron Letters. 2014;55(36):5014-8.
3. Khalil NA, Ahmed EM, Mohamed KO, Nissan YM, Zaitone SA-B. Synthesis and biological evaluation of new pyrazolone–pyridazine conjugates as anti-inflammatory and analgesic agents. Bioorganic & Medicinal Chemistry. 2014;22(7):2080-9.
4. Mazimba O, Wale K, Loeto D, Kwape T. Antioxidant and antimicrobial studies on fused-ring pyrazolones and isoxazolones. Bioorganic & Medicinal Chemistry. 2014;22(23):6564-9.
5. Sivakumar KK, Rajasekaran A, Senthilkumar P, Wattamwar PP. Conventional and microwave assisted synthesis of pyrazolone Mannich bases possessing anti-inflammatory, analgesic, ulcerogenic effect and antimicrobial properties. Bioorganic & Medicinal Chemistry Letters. 2014;24(13):2940-4.
6. Mor S, Sindhu S. Synthesis, Type II diabetes inhibitory activity, antimicrobial evaluation and docking studies of indeno[1,2-c]pyrazol-4(1H)-ones. Medicinal Chemistry Research. 2019;29(1):46-62.
7. Mor S, Mohil R, Nagoria S, Kumar A, Lal K, Kumar D, et al. Regioselective Synthesis, Antimicrobial Evaluation and QSAR Studies of Some 3-Aryl-1-heteroarylindeno[1,2-c] pyrazol-4(1H)-ones. Journal of Heterocyclic Chemistry. 2016;54(2):1327-41.
8. Rostom SAF. Synthesis and in vitro antitumor evaluation of some indeno[1,2-c]pyrazol(in)es substituted with sulfonamide, sulfonylurea(-thiourea) pharmacophores, and some derived thiazole ring systems. Bioorganic & Medicinal Chemistry. 2006;14(19):6475-85.
9. Ahsan MJ, Khalilullah H, Stables JP, Govindasamy J. Synthesis and anticonvulsant activity of 3a,4-dihydro-3H-indeno[1,2-c]pyrazole-2-carboxamide/carbothioamide analogues. Journal of Enzyme Inhibition and Medicinal Chemistry. 2012;28(3):644-50.
10. Bayat M, Nasri S. A Simple and Environmentally Benign Synthetic Protocol of Indeno-Fused Pyrido[2,3-d]pyrimidines. Journal of Heterocyclic Chemistry. 2017;54(6):3389-94.
11. Singh K. Applications of Indan-1,3-Dione in Heterocyclic Synthesis. Current Organic Synthesis. 2016;13(3):385-407.
12. Kaur N, Kumar A, Singh K. Synthesis of Novel Indenopyrimidine Sulfonamides from Indenopyrimidine-2-Amines via S–N Bond Formation. Polycyclic Aromatic Compounds. 2020:1-14.
13. Mor S, Sindhu S, Nagoria S, Khatri M, Garg P, Sandhu H, et al. Synthesis, Biological Evaluation, and Molecular Docking Studies of SomeN-thiazolyl Hydrazones and Indenopyrazolones. Journal of Heterocyclic Chemistry. 2019;56(5):1622-33.
14. Zang H, Su Q, Mo Y, Cheng B. Ionic liquid under ultrasonic irradiation towards a facile synthesis of pyrazolone derivatives. Ultrasonics Sonochemistry. 2011;18(1):68-72.
15. Sobhani S, Hasaninejad A-R, Maleki MF, Parizi ZP. Tandem Knoevenagel–Michael Reaction of 1-Phenyl-3-methyl-5-pyrazolone with Aldehydes Using 3-Aminopropylated Silica Gel as an Efficient and Reusable Heterogeneous Catalyst. Synthetic Communications. 2012;42(15):2245-55.
16. Wang W, Wang SX, Qin XY, Li JT. Reaction of Aldehydes and Pyrazolones in the Presence of Sodium Dodecyl Sulfate in Aqueous Media. Synthetic Communications. 2005;35(9):1263-9.
17. Niknam K, Saberi D, Sadegheyan M, Deris A. Silica-bonded S-sulfonic acid: an efficient and recyclable solid acid catalyst for the synthesis of 4,4′-(arylmethylene)bis(1H-pyrazol-5-ols). Tetrahedron Letters. 2010;51(4):692-4.
18. Akondi AM, Kantam ML, Trivedi R, Bharatam J, Vemulapalli SPB, Bhargava SK, et al. Ce/SiO2 composite as an efficient catalyst for the multicomponent one-pot synthesis of substituted pyrazolones in aqueous media and their antimicrobial activities. Journal of Molecular Catalysis A: Chemical. 2016;411:325-36.
19. Hosseinzadeh Z, Piryaei M, Babashpour Asl M, Abolghasemi MM. ZnO polythiophene SBA-15 nanoparticles as a solid-phase microextraction fiber for fast determination essential oils of Matricaria chamomilla. Nanochemistry Research. 2018;3(2):124-30.
20. Rostamnia S, Doustkhah E. Sulfonic-Based Precursors (SAPs) for Silica Mesostructures: Advances in Synthesis and Applications. Nanochem Res. 2016;1(1):19-32.
21. Atashin H, Malakooti R. Magnetic iron oxide nanoparticles embedded in SBA-15 silica wall as a green and recoverable catalyst for the oxidation of alcohols and sulfides. Journal of Saudi Chemical Society. 2017;21:S17-S24.
22. Appaturi JN, Johan MR, Ramalingam RJ, Al-Lohedan HA. Highly efficient green mesostructured urea functionalized on SBA-15 catalysts for selective synthesis of benzlidenemalononitrile. Microporous and Mesoporous Materials.

2018;256:67-74.
23. Golchin Hosseini H, Rostamnia S. Post-synthetically modified SBA-15 with NH2-coordinately immobilized iron-oxine: SBA-15/NH2-FeQ3 as a Fenton-like hybrid catalyst for the selective oxidation of organic sulfides. New Journal of Chemistry. 2018;42(1):619-27.
24. Safaei-Ghomi J, Bakhtiari A. Tungsten anchored onto functionalized SBA-15: an efficient catalyst for diastereoselective synthesis of 2-azapyrrolizidine alkaloid scaffolds. RSC Advances. 2019;9(34):19662-74.
25. Vengatesan MR, Devaraju S, Dinakaran K, Alagar M. SBA-15 filled polybenzoxazine nanocomposites for low-k dielectric applications. Journal of Materials Chemistry. 2012;22(15):7559.
26. Bendahou K, Cherif L, Siffert S, Tidahy HL, Benaïssa H, Aboukaïs A. The effect of the use of lanthanum-doped mesoporous SBA-15 on the performance of Pt/SBA-15 and Pd/SBA-15 catalysts for total oxidation of toluene. Applied Catalysis A: General. 2008;351(1):82-7.
27. Graf N, Yegen E, Gross T, Lippitz A, Weigel W, Krakert S, et al. XPS and NEXAFS studies of aliphatic and aromatic amine species on functionalized surfaces. Surface Science. 2009;603(18):2849-60.
28. Hess C, Tzolova-Müller G, Herbert R. The Influence of Water on the Dispersion of Vanadia Supported on Silica SBA-15: A Combined XPS and Raman Study. The Journal of Physical Chemistry C. 2007;111(26):9471-9.
29. Yavari I, Seyfi S, Skoulika S. A Convenient Synthesis of Functionalized Indenopyrazolones from Indan-1,2,3-trione, Benzaldehydes, and Phenylhydrazine. Helvetica Chimica Acta. 2012;95(9):1581-5.
30. Pilipecz MV, Mucsi Z, Nemes P, Scheiber P. Chemistry of nitroenamines. Synthesis of pyrrolizine derivatives. Heterocycles. 2007;71(9):1919-28.
31. Lobo G, Zuleta E, Charris K, Capparelli MV, Briceño A, Angel J, et al. Synthesis and Crystal Structure of (4bRS,9bRS)-5-(2,4-dimethoxyphenyl)-4b,9b-7,7-dimethyldihydroxy-4b,5,6,7,8,9b-hexahydroindeno[1,2-b]indole-9,10-dione. Journal of Chemical Research. 2011;35(4):222-4.